Clin Orthop Relat Res (2008) 466:977–984
DOI 10.1007/s11999-008-0117-7

ORIGINAL ARTICLE

Self-assembled Monolayer Films of Phosphonates for Bonding RGD to Titanium

Andras Heijink MD, Jeffrey Schwartz PhD, Mark E. Zobitz MS, K. Nicole Crowder MS, Gregory E. Lutz MD, Jean D. Sibonga PhD

Received: 24 April 2007 / Accepted: 24 December 2007 / Published online: 26 January 2008

Abstract Modification of the implant surface with the Arg-Gly-Asp tripeptide (RGD) putatively facilitates osteoblast attachment for improved implant fixation in the laboratory. We compared the histomorphometric and mechanical performance of titanium implants coated with RGD using a novel interface of self-assembled monolayers of phosphonates (RGD/SAMP) and implants coated with RGD using the more conventional thiolate-gold interface (RGD/thiolate-gold). We hypothesized RGD/SAMP-coated implants would show greater bone ongrowth and implant fixation than RGD/thiolate-gold-coated ones. We implanted an RGD/SAMP-coated implant in one femur and an RGD/thiolate-gold-coated in the contralateral femur of 60 rats. At 2, 4, and 8 weeks after implantation, 10 rats were sacrificed for histologic evaluation and another 10 for biomechanical testing. Bone-implant ongrowth and implant force-to-failure of the two implants were similar at all times. Although RGD/SAMP-coated implants did not show superior bone ongrowth and implant fixation, RGD/SAMP-coated implants have at least equally good histomorphometric and mechanical in vivo performance as RGD/thiolate-gold-coated ones. Additional in vivo characterization of self-assembled monolayer films of phosphonates as interface to bond RGD to titanium is needed to explore its full potential and seems justified based on the results of this study.

Each author certifies that he or she has no commercial associations (eg, consultancies, stock ownership, equity interest, patent/licensing arrangements, etc) that might pose a conflict of interest in connection with the submitted article.
Each author certifies that his or her institution has approved the animal protocol for this investigation and that all investigations were conducted in conformity with ethical principles of research.

A. Heijink (✉), M. E. Zobitz
Biomechanics Laboratory, Division of Orthopedic Research, Mayo Clinic, Rochester, MN 55905, USA
e-mail: heijink.andras@mayo.edu

A. Heijink
Department of Orthopedic Surgery, Mayo Clinic, Rochester, MN, USA

J. Schwartz, K. Nicole Crowder
Department of Chemistry, Princeton University, Princeton, NJ, USA

G. E. Lutz
Department of Physiatry, Hospital for Special Surgery, New York, NY, USA

J. D. Sibonga
Bone Histomorphometry Laboratory, Mayo Clinic, Rochester, MN, USA

Introduction

Bone ongrowth onto the implant surface enhances implant fixation and improves resistance to migration of particles with osteolytic potential [21, 30, 50]. Various surface coatings and texturing techniques have been studied for their potential to enhance this bone ongrowth [2, 5, 16, 21, 28, 33, 45, 49]. With these techniques anchorage-dependent cells, such as osteoblasts, must adhere to a surface to survive and perform subsequent cellular functions [4, 27]. Adhesion of such cells to the extracellular matrix of bone involves cell attachment and spreading, organization of the cytoskeleton, and formation of focal adhesions [1, 39]. Extracellular matrix proteins play a regulatory role in these processes. Only after successful adhesion will the osteoblast go through its subsequent stages of development in the process of osteogenesis: proliferation and synthesis of extracellular matrix, matrix maturation and organization, and matrix mineralization [46, 47].

Cell-extracellular matrix and cell-cell interactions are complex and occur in large part through interaction of specific amino acid sequences, particularly the tripeptide Arg-Gly-Asp (RGD) [7, 17, 22, 24, 32, 35, 36, 48], with integrins on the surface of osteoblasts and on other cells [4, 25, 40]. Binding of RGD also plays a major role in osteoblast function and development, attachment [8, 9, 26, 27, 37, 39], cell spreading [39], proliferation [27], migration [8], extracellular matrix production [26], and mineralization [9, 26]. Accordingly, considerable effort has been made to bond RGD to implant surfaces in model systems [8, 9, 26, 27, 35, 36, 39] to enhance osteoblast attachment and subsequent bone ongrowth in vivo [12–14, 41].

Titanium implants are naturally coated with a surface oxide that is chemically resistant; therefore, an interface must be created on the implant surface to enable further bonding of organics to such implants. The currently accepted standard interface is the thiolate-gold interface. This interface reportedly decomposes in air over several days [15, 29, 42, 52]. A novel interface of self-assembled monolayer films of phosphonates (SAMP) is mechanically strong and chemically stable in air, while enabling high surface coverage by organics [19, 20]. In particular, SAMP have been used to couple RGD to titanium to promote cell attachment in vitro [18, 43].

We hypothesized RGD/SAMP-coated implants would show greater bone ongrowth, measured as bone-pin contact, than RGD/thiolate-gold-coated ones and better implant fixation, measured as implant force-to-failure.

Material and Methods

We implanted an RGD/thiolate-gold-coated smooth titanium rod (15.0 mm × 1.6 mm) in one femur and an RGD/SAMP-coated one in the contralateral femur of 60 male Sprague- Dawley rats (Harlan Co, Indianapolis, IN). All rats were 12 weeks of age at the time of implantation and had an average mass of 382 ± 41 g (range, 285–466 g). The animals were administered the bone fluorochromes calcein (20 mg/kg) and tetracycline HCl (20 mg/kg) at two distinct times to enable calculations of bone formation and mineralization rates. At 2, 4, and 8 weeks after implantation, 10 animals were sacrificed for histomorphometric analysis (Group I) and 10 for mechanical testing (Group II). Assuming the analysis was simplified to a paired comparison, with 30 animals with complete data, we would be able to detect an effect size of 0.53. We considered an effect size of 1.0 biologically meaningful. The analysis takes advantage of the paired nature of the data when possible (complete data) and thus was able to detect a slightly larger effect size than estimated here. Approval was obtained from the Institutional Animal Care and Use Committee at the Mayo Clinic, Rochester, MN. NIH guidelines for the care and use of laboratory animals were observed.

Titanium alloy (Ti-6Al-4V) rods, 1.6 mm in diameter, were hand-sanded using sandpaper coated with 240, 500, 800, and 1200 grit SiC. The titanium rods were washed with sonication in dichloromethane (30 minutes), then methyl ethyl ketone (30 minutes), and then methanol (three 15-minute intervals). Then, the titanium rods were covalently coated with RGD.

For the RGD/thiolate-gold group, the rods were coated using an Edwards Coating System (Edwards, Inc, Wilmington, MA) at reduced pressure. A layer of chromium (approximately 100 Å) was deposited followed by a layer of gold (approximately 1000 Å). Thickness of the deposited layers was monitored using a quartz crystal microgravimetry crystal located in the evaporating chamber. The rods then were cut into 15.0-mm pins and cleaned by washing with sonication in acetone (45 minutes) followed by the solvent-washing regimen as described previously. After solvent cleaning, all samples were placed in an oven at 120° C for at least 1 hour until needed. The pins then were immersed in a 0.5 mmol/L solution of RGDC peptide (Arg-Gly-Asp-Cys) in Milli-Q® water (Milli-Q® Ultrapure Water Purification System; Millipore Corp, Bellerica, MA) with a final solution pH of 6.5. Containers were covered, and the pins were allowed to react with the RGDC for 24 hours with stirring. The pins then were rinsed briefly with sonication in Milli-Q® water and were blown dry with nitrogen. For the RGD/SAMP group, the titanium rods were cut into 15.0-mm pins, which were cleaned by washing with sonication in acetone (45 minutes) and then by the solvent-washing regimen as described previously. They then were coated with SAMP of 11-hydroxyundecylphosphonic acid (PUL; 1) and converted to RGD-SAMP as previously described [18]. Quartz crystal microgravimetry showed the amounts of RGD bound to the SAMP interface or to thiolate-gold were comparable (0.22 nmol/cm^2 for the SAMP and 0.25 nmol/cm^2 for the thiolate-gold) [18].

After modification with RGD, both sets of pins were sterilized with ethylene oxide at 55° C for 3 hours after which they were kept in an oven for 10.5 hours to allow the excess ethylene oxide to evaporate. The RGD/SAMP system is stable to ethylene oxide sterilization [44]. All pins were stored at room temperature.

We anesthetized the rats with a ketamine hydrochloride/xylazine hydrochloride mixture (90/10 mg/kg) and provided analgesia with one intramuscular injection of buprenorphine hydrochloride (0.02–0.1 mg/kg), the rats' legs were shaved and disinfected with Betadine® (Purdue Pharma LLP, Stamford, CT) (30% solution). The knee was opened and the patella was released and subluxated

laterally. The intercondylar notch of the femur was broached using an 18-gauge needle (1.02 mm/0.04 inch). The femoral canal was reamed sequentially with 18- and 16-gauge needles (1.29 mm/0.05 inch). The pin was inserted past the cortex of the femoral condyles so it was fully contained in the medullary canal. Then the patella was reduced and the patellar tendon was repaired with resorbable sutures (Vicryl™ 1/0; Ethicon Inc, Somerville, NJ). The skin was closed with 9-mm cutaneous staples (Becton Dickinson and Co, Parsippany, NJ). Correct intramedullary placement of the pin was confirmed using fluoroscopy. Postoperatively, analgesia was obtained with shots of buprenorphine hydrochloride (0.02–0.1 mg/kg) every 12 hours for 3 days. Immediate weightbearing was allowed and food and water were available ad libitum. We sacrificed the animals by intraperitoneal injection of an overdose of pentobarbital (1 mL).

We evaluated interfacial shear strength by means of push-out testing. After determining the position of the pin in the specimen with fluoroscopy, the femur was cut just proximal and distal to the pin using a rotating blade. The specimen then was aligned visually in the servohydraulic testing machine (MTS, Minneapolis, MN) and held in place with a clamp. A metal rod (1 mm in diameter) was used to push out the pin at a rate of 0.1 mm/second. Force and displacement data were recorded with a personal computer. A typical force-displacement curve shows a sharp peak force when the metal rod contacted the implanted pin followed by a sharp decline (force-to-failure). We confirmed with real-time fluoroscopy implant failure occurs at this point. We excluded 10 RGD/SAMP (test) and 5 RGD/thiolate-gold-coated (control) pins from the analysis that did not follow this typical pattern because they likely indicate the implant was aligned improperly in the medullary canal. The force to produce implant failure was expressed in Newtons [10].

Two groups of specimens were available for histomorphometric analysis. Group I consisted of specimens that were per protocol assigned to histomorphometry and consequently yielded tissue sections containing implants. From these Group I specimens, 20- to 30-μm-thick longitudinal sections were prepared with the Exakt Sectioning and Grinding System (Exakt Apparatenbau GmbH, Norderstedt, Germany) after the specimens had been fixed (70% alcohol), dehydrated (90% ethanol), and embedded without demineralization in a mixture of methylmethacrylate: 2-hydroxymethacrylate (12.5:1). These sections then were stained with toluidine blue. Group II consisted of specimens that were per protocol reserved for mechanical testing and consequently yielded tissue sections without implant; these specimens had been wrapped in saline-soaked gauze (physiologic 0.9% sodium chloride) after mechanical testing and frozen at −20° C. From these Group II specimens, 5-μm-thick longitudinal sections were prepared with a Reichert-Jung microtome (Leica Microsystems, Wetzlar, Germany). These sections were stained with Trichrome-Masson stain for identification of mineralized and unmineralized bone and mounted unstained for measurement of fluorochrome labels. We could not obtain tissue-quality slides from Group II specimens at the 2-week point, presumably because of poor quality of bone present at that time; therefore we obtained histologic evaluation only for the toluidine-stained slides (Group I). Older, mineralized, lamellar bone displayed osteocytes surrounded by a lavender-stained bone matrix. Newer, less mineralized bone stained blue; it lacked the presence of osteocytes and displayed a woven pattern of bone formation instead of the organized lamellar bone structure as seen with the older bone. Histomorphometric evaluation involved measurement of the following parameters using the OsteoMeasure™ semiautomatic image analysis system (OsteoMetrics, Inc, Atlanta, GA): bone-pin contact (a measure for bone ongrowth onto the implant) and bone/medullary cavity were measured on toluidine-stained sections from Group I; and fibrous tissue interposition and fibrous tissue width were measured on Trichrome-Masson-stained sections from Group II (Table 1) [34].

The primary analysis examined the two outcomes of bone-pin contact and implant force-to-failure. Secondary analysis examined bone/medullary cavity, fibrous tissue interposition, and fibrous tissue width. Each analysis was a two-factor analysis of variance model, the factors being time of sacrifice and the interface (SAMP or thiolate-gold), this last factor being a repeated factor (using two femurs in the same rat). The analysis was performed using the SAS®

Table 1. Definitions of relevant histomorphometric parameters

Parameter	Definition
Bone-pin contact	Percentage of the implant surface covered with newly formed bone, regardless of the presence of interposing fibrous tissue
Bone/medullary cavity	Percentage of the medullary cavity area occupied with bone
Fibrous tissue interposition	The extent of fibrous tissue interposing between the newly formed bone covering the implant and the implant surface, expressed as percentage of newly formed bone adjacent to the implant covered with fibrous tissue
Fibrous tissue width	Average width of the fibrous tissue interposing between the newly formed bone covering the implant and the implant surface, expressed in micrometers

PROC MIXED (SAS Institute Inc, Cary, NC) because not all rats had measurements for both interfaces. For the implant force-to-failure measurement, 18 of 25 rats had complete data (both interfaces); for bone area/bone marrow area and bone-pin contact measurements, 26 of 31 rats had complete data; and for fibrous tissue interposition and fibrous tissue width, nine of 17 rats had complete data. Examining the differences (difference between the two implants in one animal) in interfaces for rats with complete data gave rise to similar conclusions.

Results

Bone ongrowth, expressed as bone-pin contact, was similar ($p = 0.10$) for implants coated with RGD using the SAMP interface (RGD/SAMP) and implants coated with RGD using the thiolate-gold interface (RGD/thiolate-gold) at all times (Table 2). The difference between the two coatings did not depend ($p = 0.27$) on survival time. There was, however, an increase ($p < 0.001$) in overall bone ongrowth with increasing survival time. Most of the 2-week slides showed woven bone in the medullary cavity that bridged the gap between the implant surface and the endocortical perimeter (in nine of 10 RGD/SAMP specimens and in six of nine RGD/thiolate-gold specimens that rendered slides of sufficient quality) (Fig. 1). The 4-week slides showed similar bridging with woven bone (in five of eight RGD/SAMP specimens and in eight of nine RGD/thiolate-gold specimens that rendered slides of sufficient quality). The 8-week slides showed smaller amounts of woven bone with no evidence of bridging in any of the slides (in zero of 10 RGD/SAMP specimens and in zero of 10 RGD/thiolate-gold specimens). Instead, there were more lavender-stained, mineralized bone trabeculae that were aligned and juxtaposed to the implant surface. In the majority of the specimens, there was fibrous tissue interposed between the implant surface and the newly formed bone covering the implant (for the 4-week point, in three of five RGD/SAMP specimens and in five of eight RGD/thiolate-gold specimens; and for the 8-week point, in four of six RGD/SAMP specimens and in six of seven RGD/thiolate-gold specimens that rendered slides of sufficient quality; 2-week specimens not available for this group) (Figs. 2, 3).

Table 2. Histomorphometry results

Parameter	Survival time (weeks)	Interface platform	
		SAMP	Thiolate-Gold
Bone-pin contact (%)	2	20.1 (6.1)	19.5 (6.8)
	4	46.1 (6.4)	40.9 (6.8)
	8	58.0 (6.1)	38.6 (6.5)
Bone/medullary cavity (%)	2	18.6 (1.6)*	10.2 (1.7)*
	4	17.2 (1.7)	16.4 (1.7)
	8	12.0 (1.6)	11.9 (1.6)
Fibrous tissue interposition (%)	2	NA	NA
	4	16.2 (13.1)	26.4 (8.9)
	8	22.1 (12.3)	17.8 (8.9)
Fibrous tissue width (μm)	NA	NA	NA
	4	14.1 (12.2)	29.6 (8.0)
	8	12.4 (11.5)	23.3 (7.9)

Values are least-squares mean, with standard error of the mean in parentheses; * denotes significance between groups ($p = 0.04$); SAMP = self-assembled monolayers of phosphonates; NA = not available.

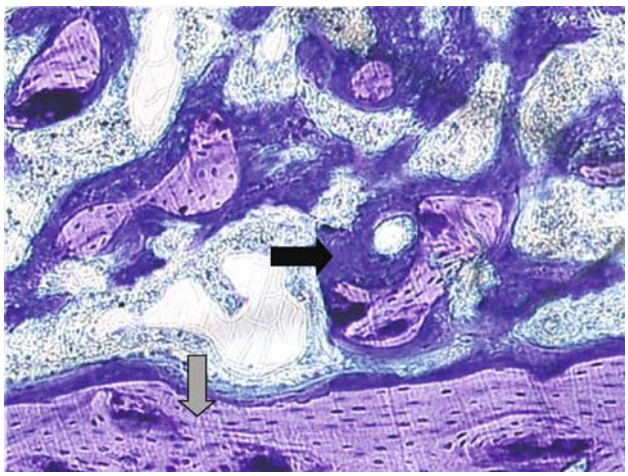

Fig. 1 The photomicrograph shows a longitudinal section through a 2-week specimen containing an RGD/SAMP-coated implant (implant not shown). The lavender-stained areas represent older, more mineralized bone (grey arrow); the blue-stained areas represent newer, less mineralized bone (black arrow) (Stain, toluidine blue; original magnification, ×10).

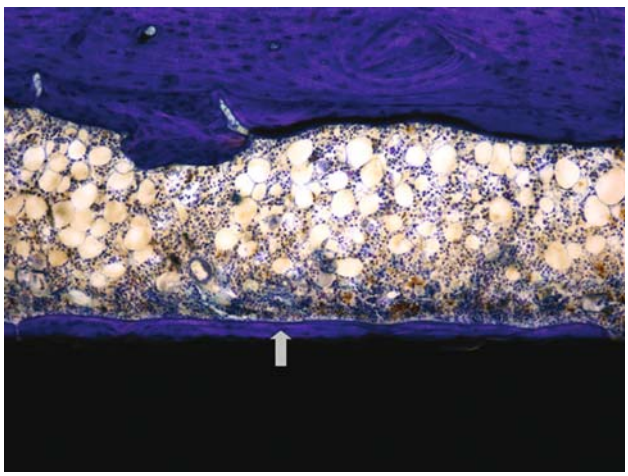

Fig. 2 The photomicrograph shows a longitudinal section through an 8-week specimen containing an RGD/SAMP-coated implant (black area). Newly formed bone (gray arrow) is observed directly adjacent to the implant, without interposition of fibrous tissue (Stain, toluidine blue; original magnification, ×100).

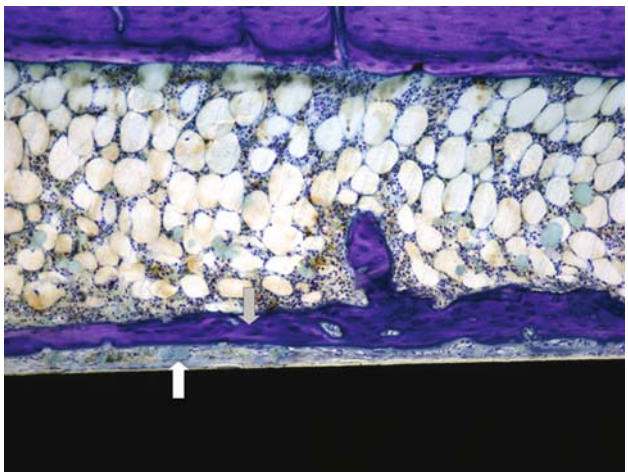

Fig. 3 The photomicrograph shows a longitudinal section through an 8-week specimen containing an RGD/SAMP-coated implant (black area). Fibrous tissue interposition (white arrow) is observed between the implant surface and the newly formed bone adjacent to the implant (gray arrow) (Stain, toluidine blue; original magnification, ×100).

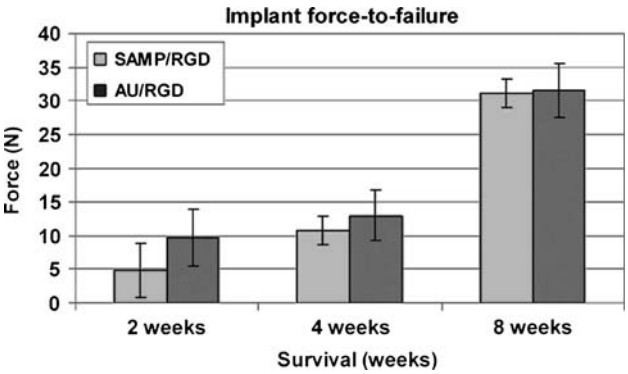

Fig. 4 A histogram shows implant force-to-failure with time. Values are least-squares mean (± standard error). There was no difference in force-to-failure between RGD/SAMP- and RGD/thiolate-gold (AU)-coated implants at any time.

Implant fixation was similar ($p = 0.44$) for implants coated with RGD using the SAMP interface (RGD/SAMP) and implants coated with RGD using the thiolate-gold interface (RGD/thiolate-gold) at all times (Fig. 4). The difference between the two coatings did not depend ($p = 0.79$) on survival time. Overall implant fixation increased ($p < 0.001$) with increasing survival time.

Secondary analysis suggested the extent and the width (ie, thickness) of the fibrous tissue interposition between the implant and the newly formed bone covering the implant were similar for the two coatings at either 4 or 8 weeks ($p = 0.31$ and $p = 0.84$, respectively) and without an increase from 4 to 8 weeks for either one ($p = 0.48$ and $p = 0.69$, respectively) (Table 2). Bone area/bone marrow area was greater for implants coated with RGD/SAMP than implants coated with RGD/thiolate-gold at 2 weeks ($p = 001$), but not at 4 and 8 weeks ($p = 0.73$ and $p = 0.96$, respectively) (Table 2).

Discussion

Surface modification of orthopaedic implants with RGD to enhance bone ongrowth and subsequent implant fixation has been studied in vitro and in vivo [8, 11, 26, 27, 31, 35, 36, 38, 51]. Coating of titanium implants with RGD requires a chemically stable interface. The current accepted standard, a thiolate-gold interface, decomposes in a few days. We therefore explored a novel SAMP interface, which is chemically stable for longer duration, with implants coated with RGD using the thiolate-gold interface. We hypothesized, because of its superior chemical stability in air, implants coated with RGD using this novel SAMP interface would show greater bone ongrowth and implant fixation.

Some limitations of this study reduce the power of our study to interpret findings and detect differences. This study did not include comparison of RGD/SAMP-coated with uncoated implants to allow for paired comparison and more powerful interpretations. Because implants coated with RGD using the gold-thiolate interface show enhanced implant osseointegration compared with uncoated titanium implants, we believe the current study design allows for a sound characterization of RGD/SAMP-coated implants [14]. Not all specimens yielded sections of satisfactory quality for analysis; this limits our power to detect differences between the two groups. Assuming the analysis was simplified to a straightforward paired comparison, post hoc estimation tells us we had 80% power to detect an effect size of 0.60 for bone-pin contact and an effect size of 0.75 for force-to-failure. We did not include surface analysis of the implants with time; this would have provided direct information about the chemical stability of both interfaces. Other limitations are thought to affect the results for both groups equally and therefore are less likely to bias the results; they may, however, complicate comparison with other studies. Despite using the same model, surgical technique, and implant size as those described by Ferris et al. [14], we did not obtain perfect press-fit placement of all implants; if the implant is not press-fit at Time Zero, osteoblasts first need to migrate to the implant surface, and bone ongrowth may be delayed and thus reduced as a function of survival time. Resection of the proximal and distal parts of the femur during preparation of the specimen for push-out testing could have damaged the microstructure of the newly formed bone surrounding the implant, which could result in underestimation of implant fixation. Push-out testing carries the risk of suboptimal alignment of the load application with a subsequent increase in friction,

which may result in overestimation of the push-out force. Evaluation of bone bridging of the gap between the implant surface and the endocortical perimeter is influenced by the orientation of the implant in the femoral canal and of the sectioning plane in relation to the implant axis; analysis of oblique sections or obliquely oriented implants may result in over- or underestimation of bone ingrowth. In addition, correlations between histologic findings and mechanical data should be interpreted with caution; implant fixation is dependent on bone bridging of the gap between the implant surface and the endocortical surface and also on the amount and the quality of the bone bridging the gap [41]. These parameters are not possible to quantify for the entire implant surface with a two-dimensional presentation such as a histologic slide. Finally, comparison of in vivo studies is complicated because of important differences in study design: different animal models, implantation sites, implant materials and surfaces, and RGD characteristics and survival times [12, 13]. Despite these limitations, we believe the design allows comparison between the RGD/SAMP- and RGD/thiolate-gold-coated implants per se.

Levels of RGD peptide loading on the titanium alloy and gold surfaces were comparable (22 nmol/cm^2 for the SAMP interface and 0.25 nmol/cm^2 for the gold-thiolate interface), as measured by quartz crystal microgravimetry, using a procedure developed to allow dynamic measurements of surface loading [18]. Whereas the gold-thiolate interface decomposes in vitro during a period of several days [15, 29, 42, 52], the SAMP interface remains stable for a longer period of time [44]. Despite this comparable RGD content in combination with superior chemical stability of the SAMP interface, implant bone coverage of RGD/SAMP-coated implants, considered regardless of interposing fibrous tissue, was not different from RGD/thiolate-gold-coated implants. The total amount of bone formation in the marrow space around the implant was greater with the RGD/SAMP-coated pins than with the RGDC/thiolate-gold-coated ones at 2 weeks, but not at the later times. Although the interpretation of this finding is not completely clear, it could suggest a larger initial osteoblast attracting potential of the RGD/SAMP system, possibly because of prolonged chemical stability of the RGD/SAMP coating.

At 2 weeks, there was bone bridging of the gap between the implant and endocortical surface in most of the specimens. Although with the RGD/SAMP-coated implants there was considerably more bone formation in this gap at 2 weeks than with the gold-thiolate interface, the immaturity of this bone, which renders it relatively weak compared with mature bone, could explain the lack of difference in mechanical performance at this time [41]. Although bridging of the gap was observed at 4 weeks, the amount of bone was not different between the two interfaces. This could explain why we observed no mechanical difference at this time. At 8 weeks, there was no bridging observed in any of the specimens and a mechanical difference thus would seem less likely. Although there was no difference in implant force-to-failure between the two interfaces at any time, there was an increase in the force-to-failure with lengthening of the survival time, particularly from 4 to 8 weeks, despite a decrease in the amount of bone between the implant and the cortical inner perimeter from 4 to 8 weeks and the absence of bridging at 8 weeks. This increase in implant force-to-failure with time has been reported and is suggestive of progressive osseointegration with time [3, 14]. A temporary reduction in bone-implant contact between 3 and 28 days after implantation has been reported, which has been contributed to installation trauma, inflammation, and removal of injured bone tissue at the interface [3, 10].

The majority of specimens showed fibrous tissue interposition between the implant surface and the newly formed bone covering the implant. The extent and width of this fibrous tissue layer were not different for the RGD/SAMP- and RGD/thiolate-gold-coated implants. This fibrotic layer could at least in part account for the nonspecific effect of surface coating on implant force-to-failure by acting as a barrier to bone ongrowth. The RGD tripeptide not only fosters osteoblast attachment [8, 9, 26, 27, 37, 39] but also interacts with other cells, including fibroblasts [22, 31, 35]. Also, micromotion of orthopaedic implants is associated with the development of an interposed fibrous membrane.

The SAMP interface does have a mechanical strength advantage over the thiolate-gold interface. The mechanical shear strength of the SAMP interface on titanium (a bulk materials property) is 52.1 $\pm$ 2.1 MPa [6]. No comparable measurement of the shear strength of an alkanethiolate film on gold has been reported, but the force associated with rupturing a discrete, molecular gold-thiolate bond has been measured as 1.4 $\pm$ 0.3 nN [23]. To compare bulk mechanical properties of the SAMP on titanium with molecular ones for the alkanethiolate on gold, it is necessary to convert the interfacial shear strength of the SAMP accordingly to a molecular basis. The surface loading for a PUL film on titanium has been measured by quartz crystal microgravimetry to be 1.00 $\pm$ 0.09 nmol/cm^2; thus, the shear strength of the film on titanium, on a molecular basis, is 8.65 $\times$ 10^{-8} Pa, or 86.5 nN[6], which is greater than the thiolate-gold interface. We did not address the failure mode of the implants, at the implant-interface bond or at the coating-surrounding tissue bond (bone or fibrous) interface. As long as this failure mode is not known, the importance of the biomechanical strength advantage of the RGD/SAMP system remains unclear.

We evaluated the in vivo performance of a newly developed interface of SAMP to bond the tripeptide RGD to

the Ti-6Al-4V surface and compared its performance with that of the more conventional gold-thiolate interface. Although the RGD/SAMP-coated implants did not show superior bone ongrowth and implant fixation, as was hypothesized, RGD/SAMP-coated implants have shown equally good histomorphometric and mechanical performance in vivo as RGD/thiolate-gold-coated ones. Continuation of in vivo characterization of the newly developed SAMP interface to bond RGD to titanium seems justified and must address comparison with an unmodified titanium surface, the importance of press-fit implant placement, direct analysis of the implant surface, and competition between fibroblasts and osteoblasts for the RGD anchor.

Acknowledgments We thank Donna Jewison for preparation of the histologic specimens.

References

1. Anselme K. Osteoblast adhesion on biomaterials. *Biomaterials*. 2000;21:667–681.
2. Bierbaum BE, Zeegen EN, Dayton MR. Hydroxyapatite coating on the femoral stem in primary total hip arthroplasty. *Orthopedics*. 2003;26:913–914.
3. Branemark R, Ohrnell LO, Nilsson P, Thomsen P. Biomechanical characterization of osseointegration during healing: an experimental in vivo study in the rat. *Biomaterials*. 1997;18:969–978.
4. Chen CS, Mrksich M, Huang S, Whitesides GM, Ingber DE. Geometric control of cell life and death. *Science*. 1997;276:1425–1428.
5. Cook SD, Thomas KA, Dalton JE, Volkman TK, Whitecloud TS 3rd, Kay JF. Hydroxylapatite coating of porous implants improves bone ingrowth and interface attachment strength. *J Biomed Mater Res*. 1992;26:989–1001.
6. Danahy MP, Avaltroni MJ, Midwood KS, Schwarzbauer JE, Schwartz J. Self-assembled monolayers of alpha,omega-diphosphonic acids on Ti enable complete or spatially controlled surface derivatization. *Langmuir*. 2004;20:5333–5337.
7. Dedhar S, Ruoslahti E, Pierschbacher MD. A cell surface receptor complex for collagen type I recognizes the Arg-Gly-Asp sequence. *J Cell Biol*. 1987;104:585–593.
8. Dee KC, Anderson TT, Bizios R. Osteoblast population migration characteristics on substrates modified with immobilized adhesive peptides. *Biomaterials*. 1999;20:221–227.
9. Dee KC, Rueger DC, Andersen TT, Bizios R. Conditions which promote mineralization at the bone-implant interface: a model in vitro study. *Biomaterials*. 1996;17:209–215.
10. Dhert WJ, Verheyen CC, Braak LH, de Wijn JR, Klein CP, de Groot K, Rozing PM. A finite element analysis of the push-out test: influence of test conditions. *J Biomed Mater Res*. 1992;26:119–130.
11. Durrieu MC, Pallu S, Guillemot F, Bareille R, Amédée J, Baquey CH, Labrugère C, Dard M. Grafting RGD containing peptides onto hydroxyapatite to promote osteoblastic cells adhesion. *J Mater Sci Mater Med*. 2004;15:779–786.
12. Elmengaard B, Bechtold JE, Soballe K. In vivo effects of RGD-coated titanium implants inserted in two bone-gap models. *J Biomed Mater Res A*. 2005;75:249–255.
13. Elmengaard B, Bechtold JE, Soballe K. In vivo study of the effect of RGD treatment on bone ongrowth on press-fit titanium alloy implants. *Biomaterials*. 2005;26:3521–3526.
14. Ferris DM, Moodie GD, Dimond PM, Gioranni CW, Ehrlich MG, Valentini RF. RGD-coated titanium implants stimulate increased bone formation in vivo. *Biomaterials*. 1999;20:2323–2331.
15. Flynn NT, Tran MJ, Cima MJ, Langer R. Long-term stability of self-assembled monolayers in biological media. *Langmuir*. 2003;19:10909–10915.
16. Frenkel SR, Jaffe WL, Dimaano F, Iesaka K, Hua T. Bone response to a novel highly porous surface in a canine implantable chamber. *J Biomed Mater Res B Appl Biomater*. 2004;71:387–391.
17. Gartner TK, Bennett JS. The tetrapeptide analogue of the cell attachment site of fibronectin inhibits platelet aggregation and fibrinogen binding to activated platelets. *J Biol Chem*. 1985;260:11891–11894.
18. Gawalt ES, Avaltroni MJ, Danahy MP, Silverman BM, Hanson EL, Midwood KS, Schwarzbauer JE, Schwartz J. Bonding organics to Ti alloys: facilitating human osteoblast attachment and spreading on surgical implant materials. *Langmuir*. 2003;19:200–204.
19. Gawalt ES, Avaltroni MJ, Koch N, Schwartz J. Self-assembly and bonding of alkanephosphonic acids on the native oxide surface of titanium. *Langmuir*. 2001;17:5736–5738.
20. Gawalt ES, Brault-Rios K, Dixon MS, Tang DC, Schwartz J. Enhanced bonding of organometallics to titanium via a titanium(III) phosphate interface. *Langmuir*. 2001;17:6743–6745.
21. Geesink RG. Osteoconductive coatings for total joint arthroplasty. *Clin Orthop Relat Res*. 2002;395:53–65.
22. Ginsberg M, Pierschbacher MD, Ruoslahti E, Marguerie G, Plow E. Inhibition of fibronectin binding to platelets by proteolytic fragments and synthetic peptides which support fibroblast adhesion. *J Biol Chem*. 1985;260:3931–3936.
23. Grandbois M, Beyer M, Rief M, Clausen-Schaumann H, Gaub HE. How strong is a covalent bond? *Science*. 1999;283:1727–1730.
24. Hayman EG, Pierschbacher MD, Ruoslahti E. Detachment of cells from culture substrate by soluble fibronectin peptides. *J Cell Biol*. 1985;100:1948–1954.
25. Hynes RO. Integrins: a family of cell surface receptors. *Cell*. 1987;48:549–554.
26. Itoh D, Yoneda S, Kuroda S, Kondo H, Umezawa A, Ohya K, Ohyama T, Kasugai S. Enhancement of osteogenesis on hydroxyapatite surface coated with synthetic peptide (EEEEEEEPRGDT) in vitro. *J Biomed Mater Res*. 2002;62:292–298.
27. Kantlehner M, Schaffner P, Finsinger D, Meyer J, Jonczyk A, Diefenbach B, Nies B, Hölzemann G, Goodman SL, Kessler H. Surface coating with cyclic RGD peptides stimulates osteoblast adhesion and proliferation as well as bone formation. *Chembiochem*. 2000;1:107–114.
28. Kusakabe H, Sakamaki T, Nihei K, Oyama Y, Yanagimoto S, Ichimiya M, Kimura J, Toyama Y. Osseointegration of a hydroxyapatite-coated multilayered mesh stem. *Biomaterials*. 2004;25:2957–2969.
29. Lee MT, Hsueh CC, Freund MS, Ferguson GS. Air oxidation of self-assembled monolayers on polycrystalline gold: the role of the gold substrate. *Langmuir*. 1998;14:6419–6423.
30. Manley MT, Capello WN, D'Antonio JA, Edidin AA, Geesink RG. Fixation of acetabular cups without cement in total hip arthroplasty: a comparison of three different implant surfaces at a minimum duration of follow-up of five years. *J Bone Joint Surg Am*. 1998;80:1175–1185.
31. Massia SP, Stark J, Letbetter DS. Surface-immobilized dextran limits cell adhesion and spreading. *Biomaterials*. 2000;21:2253–2261.
32. Oldberg A, Franzen A, Heinegard D. Cloning and sequence analysis of rat bone sialoprotein (osteopontin) cDNA reveals an Arg-Gly-Asp cell-binding sequence. *Proc Natl Acad Sci USA*. 1986;83:8819–8823.

33. Oosterbos CJ, Rahmy AI, Tonino AJ, Witpeerd W. High survival rate of hydroxyapatite-coated hip prostheses: 100 consecutive hips followed for 10 years. *Acta Orthop Scand*. 2004;75:127–133.
34. Parfitt AM, Drezner MK, Glorieux FH, Kanis JA, Malluche H, Meunier PJ, Ott SM, Recker RR. Bone histomorphometry: standardization of nomenclature, symbols, and units: report of the ASBMR Histomorphometry Nomenclature Committee. *J Bone Miner Res*. 1987;2:595–610.
35. Pierschbacher MD, Ruoslahti E. Cell attachment activity of fibronectin can be duplicated by small synthetic fragments of the molecule. *Nature*. 1984;309:30–33.
36. Pierschbacher MD, Ruoslahti E. Variants of the cell recognition site of fibronectin that retain attachment-promoting activity. *Proc Natl Acad Sci USA*. 1984;81:5985–5988.
37. Puleo DA, Bizios R. RGDS tetrapeptide binds to osteoblasts and inhibits fibronectin-mediated adhesion. *Bone*. 1991;12:271–276.
38. Rezania A, Healy KE. Integrin subunits responsible for adhesion of human osteoblast-like cells to biomimetic peptide surfaces. *J Orthop Res*. 1999;17:615–623.
39. Rezania A, Thomas CH, Branger AB, Waters CM, Healy KE. The detachment strength and morphology of bone cells contacting materials modified with a peptide sequence found within bone sialoprotein. *J Biomed Mater Res*. 1997;37:9–19.
40. Ruoslahti E, Pierschbacher MD. New perspectives in cell adhesion: RGD and integrins. *Science*. 1987;238:491–497.
41. Schliephake H, Scharnweber D, Dard M, Rössler S, Sewing A, Meyer J, Hoogestraat D. Effect of RGD peptide coating of titanium implants on periimplant bone formation in the alveolar crest: an experimental pilot study in dogs. *Clin Oral Implants Res*. 2002;13:312–319.
42. Schoenfisch MH, Pemberton JE. Air stability of alkanethiol self-assembled monolayers on silver and gold surfaces. *J Am Chem Soc*. 1998;120:4502–4513.
43. Schwartz J, Avaltroni MJ, Danahy MP, Silverman BM, Hanson EL, Schwarzbauer JE, Midwood KS, Gawalt ES. Cell attachment and spreading on metal implant materials. *Mater Sci Eng C*. 2003;23:395–400.
44. Silverman BM, Wieghaus KA, Schwartz J. Comparative properties of siloxane vs phosphonate monolayers on a key titanium alloy. *Langmuir*. 2005;21:225–228.
45. Sinha RK, Dungy DS, Yeon HB. Primary total hip arthroplasty with a proximally porous-coated femoral stem. *J Bone Joint Surg Am*. 2004;86:1254–1261.
46. Stein GS, Lian JB. Molecular mechanisms mediating proliferation/differentiation interrelationships during progressive development of the osteoblast phenotype. *Endocr Rev*. 1993;14:424–442.
47. Stein GS, Lian JB, Owen TA. Relationship of cell growth to the regulation of tissue-specific gene expression during osteoblast differentiation. *FASEB J*. 1990;4:3111–3123.
48. Suzuki S, Oldberg A, Hayman EG, Pierschbacher MD, Ruoslahti E. Complete amino acid sequence of human vitronectin deduced from cDNA: similarity of cell attachment sites in vitronectin and fibronectin. *EMBO J*. 1985;4:2519–2524.
49. Tanzer M, Gollish J, Leighton R, Orrell K, Giacchino A, Welsh P, Shea B, Wells G. The effect of adjuvant calcium phosphate coating on a porous-coated femoral stem. *Clin Orthop Relat Res*. 2004;424:153–160.
50. Urban RM, Jacobs JJ, Sumner DR, Peters CL, Voss FR, Galante JO. The bone-implant interface of femoral stems with non-circumferential porous coating. *J Bone Joint Surg Am*. 1996;78:1068–1081.
51. Verrier S, Pallu S, Bareille R, Jonczyk A, Meyer J, Dard M, Amédée J. Function of linear and cyclic RGD-containing peptides in osteoprogenitor cells adhesion process. *Biomaterials*. 2002;23:585–596.
52. Willey TM, Vance AL, van Buuren T, Bostedt C, Terminello LJ, Fadley CS. Rapid degeneration of alkanethiol-based self-assembled monolayers on gold in ambient laboratory conditions. *Surf Sci*. 2005;576:188–196.